ORIGINAL PAPER

Climatological characteristics of Bay of Bengal tropical cyclones: 1972–2017

Pankaj Bhardwaj[1] · Omvir Singh[1]

Abstract

The present study is an attempt to investigate the spatial and temporal climatology of tropical cyclone (TC) activity in the Bay of Bengal (BoB) based on the Joint Typhoon Warning Centre (JTWC) best track data for the period 1972–2017. A total of 152 TCs, with a rate of 3.30 TCs per year, were formed in the BoB during the 46-year period. A large interannual variability was witnessed in TC activity with non-significant upward or downward trend in their frequency, intensity, duration, accumulated cyclone energy (ACE), and power dissipation index (PDI). Majority of TCs were formed between the 5° N to 16° N latitudes and made their landfall over the coasts of India, Bangladesh, Myanmar, and Sri Lanka. About two-thirds of annual TCs occurred during the post-monsoon season, whereas monthly distribution exhibited a unique bimodal pattern. The number of cyclonic storms (34–47 kt) showed a slightly increasing trend, whereas intense cyclonic storms ($\geq$ 48 kt) showed a slightly decreasing trend. Additionally, about 40% and 11% of the TC events were found intensifying at 15 kt 24 h^{-1} and rapidly intensifying at 30 kt 24 h^{-1}, respectively in the BoB. It is believed that the results of the present study will update the current knowledge which will assist the scientific community as well as academicians.

1 Introduction

A tropical cyclone (TC) is the generic term for a non-frontal low pressure system of synoptic scale with organized convection over tropical or sub-tropical waters, having maximum wind speed of 34 kt or more for at least one 6-h period. These TCs are one of the most powerful and devastating weather phenomena with extreme societal and economic impacts on earth (Pielke et al. 2003, 2008; Peduzzi et al. 2012). Gray (1979) identified six important thermodynamic and dynamic factors for the formation of TCs, such as high sea surface temperature (SST) (> 26.5 °C), low magnitude of vertical wind shear (VWS), high low level vorticity, significant Coriolis force, and high mid-tropospheric relative humidity (RH). Usually, the TCs are energized by latent heat released from water vapor condensation (Rosenfeld et al. 2012). Therefore, most tropical ocean basins witness the peak occurrence of cyclones during late summer and early autumn period

when SST is high (Gutzler et al. 2013; Zhao and Raga 2015). Other factors such as the seasonal variation of the monsoon trough location are also important (Frank 1987; McBride 1995).

Historical records show that approximately 80–90 TCs in number form annually in global ocean basins (Gray 1979). The North Indian Ocean, including the BoB and the Arabian Sea, accounts for just 7% of global TCs on average (Neumann 1993). About 80% of North Indian Ocean TCs form in the BoB (IMD 2011), which tend to be the deadliest of any TCs around the globe. For example, Orissa super cyclone of 1999 resulted in about 10,000 deaths and cyclone Nargis of 2008 caused about 138,000 deaths in Myanmar (Chittibabu et al. 2004; Fritz et al. 2009). Likewise, adjoining coastal countries including Bangladesh, India, and Myanmar reported more than 75% of the casualties caused by BoB TCs (Chowdhury 2002).

Recently, researchers have extensively studied the BoB TCs activity using different approaches. Singh et al. (2001) displayed an increasing trend in the frequency of intense TCs over the North Indian Ocean. Pattanaik (2005) associated the high- and low-frequency periods of TC occurrence to the variability of large-scale atmospheric circulation, instead of SST. Besides, numerous studies have explored the impact of oceanic and atmospheric conditions on the modulation of TC activity in the

✉ Omvir Singh
  ovshome@yahoo.com

[1] Department of Geography, Kurukshetra University,
    Kurukshetra 136119, India

BoB (Ali et al. 2007; Sengupta et al. 2007; Lin et al. 2009). Singh (2008) showed the association between September and October dipole mode index (DMI) and frequency of cyclones during the month of November in the BoB. TC activity in the BoB is also strongly modulated by the tropical intraseasonal oscillation (Kikuchi and Wang 2010; Yanase et al. 2012). Girishkumar and Ravichandran (2012), Felton et al. (2013), and Bhardwaj et al. (2019a) revealed that the frequency and intensity of BoB TCs is relatively high during the La Niña than El Niño years. Ng and Chan (2012) observed a large interannual variation in the frequency of TCs over BoB. Pattanaik and Mohapatra (2016) examined the variability of cyclonic disturbances frequency over BoB to identify the suitable predictors having significant correlations with the seasonal frequency of cyclonic disturbances during October–December. Bhardwaj et al. (2019b) examined the impact of the MJO on BoB TCs activity and MJO-driven modulations in large-scale environmental conditions during the two peak TC seasons, i.e., April–June and October–December. In addition, Evan and Camargo (2011) documented the climatology of Arabian Sea cyclones despite the very less occurrence of cyclones.

The above review divulges that several studies are available pertaining to the different aspects of BoB TCs. However, most of these studies were limited for a small period, particular season and few TC parameters. A dedicated study on climatology of BoB TCs has not been undertaken as yet. Therefore, to fill this research gap, the present study has been attempted to develop a comprehensive and long-term climatology of BoB TCs (1972–2017; 46 years). The present study seeks to answer the following questions:

1. Is there a spatial variation in the formation of TCs and their tracks during different months and seasons?

2. Is there a trend in number of TCs, intensity of TCs, duration, accumulated cyclone energy (ACE), power dissipation index (PDI)?

3. Is there a difference between total distance traveled by TCs during different seasons and TCs of different intensity?

4. Is there any relationship exists between the minimum sea level pressure (MSLP) and maximum sustained wind (MSW) over BoB?

The remainder of this paper is organized as follows: Section 2 describes the datasets and the methods employed. Section 3 discusses the main results including the spatial and temporal characteristics of the TCs. Section 4 summarizes the major findings of this study.

2 Data and methodology

For North Indian Ocean, India Meteorological Department (IMD), New Delhi, and Joint Typhoon Warning Centre (JTWC), USA, provides the TCs best track data. IMD's data set provides the detailed information of location and intensity information of BoB TCs for every 6-h intervals only since 1990. However, JTWC started the satellite detection of BoB TCs for North Indian Ocean from 1972 onwards (Singh 2010). Therefore, in this study, JTWC best track data was used for the analysis of BoB TCs during 1972–2017 (46 years), available at www.npmoc.navy.mil/jtwc.html (Chu et al. 2002). This JTWC dataset is appropriate and reliable for the long-term climatological study of BoB TCs. The dataset comprises information of TCs name, position (latitude and longitude), MSLP, and 1-min MSW speed at 6-h intervals (0000, 0600, 1200, and 1800UTC). Although, World Meteorological Organization (WMO) standard for TCs is the 10-min MSW speed within a storm at an elevation of 10 m with an

Table 1 IMD's classification of cyclonic disturbances in the North Indian Ocean (Bay of Bengal and Arabian Sea) since 2015

Type	Wind speed in km/h	Wind speed in knot (mps)	Number of closed isobars at interval of 2 hPa within 5° latitude/longitude square
Low pressure area (L)	Less than 31	Less than 17 (09)	1
Depression (D)	31–49	17–27 (9–14)	2
Deep depression (DD)	50–61	28–33 (15–17)	3
Cyclonic storm (CS)	62–88	34–47 (18–24)	4–7
Severe cyclonic storm (SCS)	89–118	48–63 (25–32)	8–10
Very severe cyclonic storm (VSCS)	119–165	64–89 (33–46)	11–25
Extremely severe cyclonic storm (ESCS)	166–220	90–119 (47–61)	26–39
Super cyclonic storm (SupCS)	221 or more	120 (62) or more	40 or more

Generic names like tropical cyclone or cyclone are used to represent CS, SCS, VSCS, ESCS, and SupCS as a whole
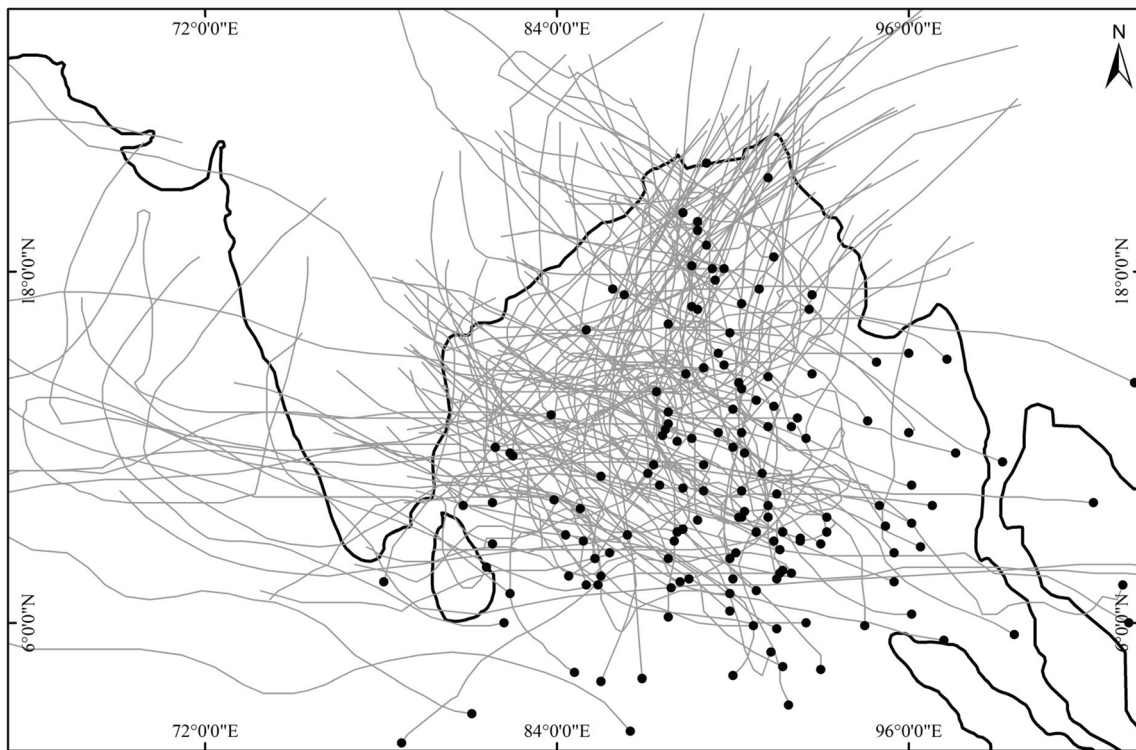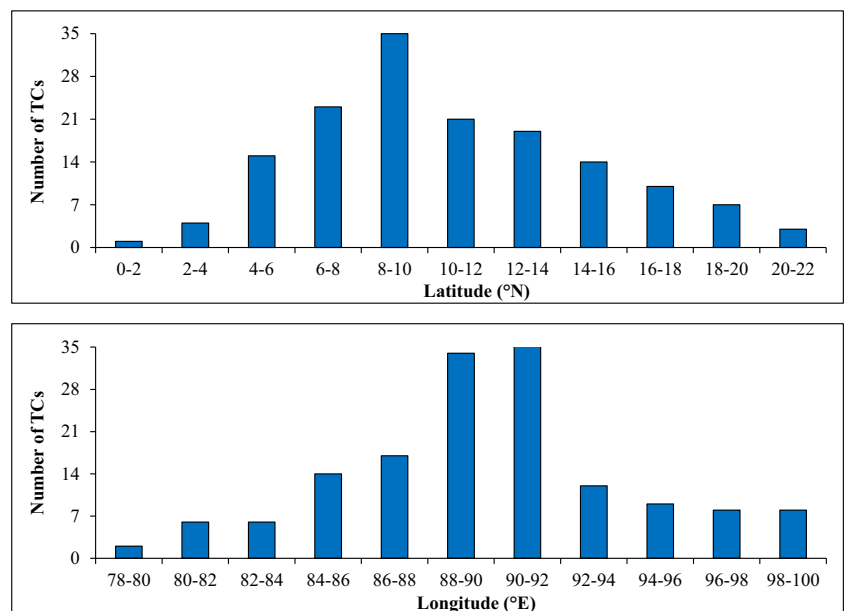
Fig. 1 Distribution of genesis locations (dots) and tracks (lines) of TCs formed in the BoB during the period 1972–2017

unobstructed surface. However, different agencies apply different time lengths such as the USA (1-min mean), IMD New Delhi (3-min mean), and Tokyo (10-min mean) for averaging MSW speed (Knapp and Kruk 2010). JTWC identified very weak and short-lived storms whose MSW speeds peaked just above 34 kt for one or two 6-hourly periods, which were not

identified in the IMD analysis. Therefore, IMD's intensity estimates are 5–10 kt lower than JTWC, which may be a result of differences in mean MSW speed period (Knapp et al. 2010). For example, as per the IMD observations, the MSW of cyclone Sidr (November 2007) and Phailin (October 2013) were 115 kt. However, in JTWC dataset, 1-min MSW of these

Fig. 2 **a** Latitudinal and **b** longitudinal distribution of TCs genesis frequency in the BoB during the period 1972–2017
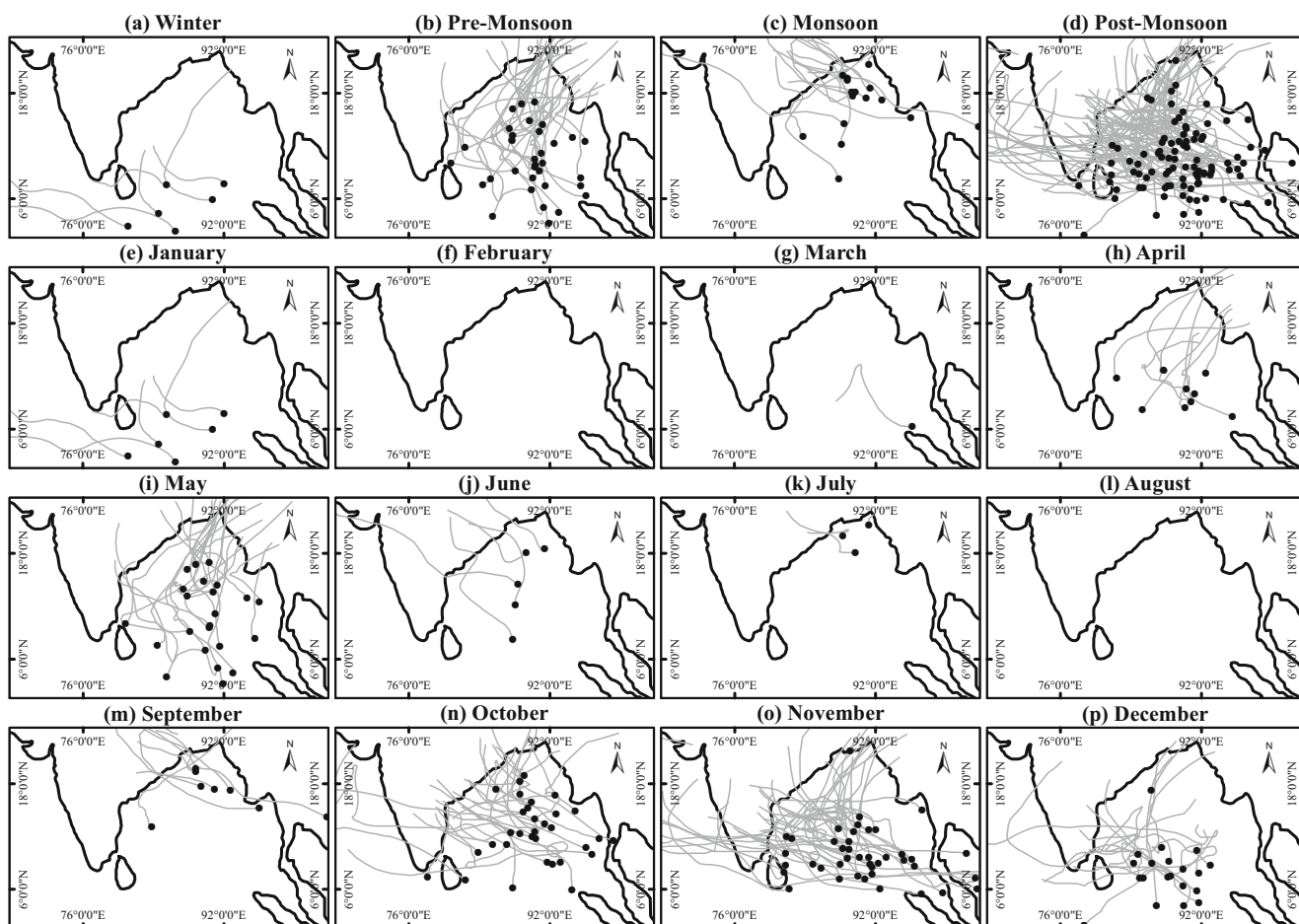
Fig. 3 **a**–**d** Seasonal and **e**–**p** monthly distribution of genesis locations (dots) and tracks (lines) of TCs formed in the BoB during the period 1972–2017

two cyclones is 140 kt (25 kt higher than IMD observations). Similarly, a cyclone was formed in April 1991 over the BoB with MSW of 140 kt (13 kt higher than IMD observations).

Table 2 Monthly mean genesis location of TCs in the BoB during the period 1972–2017

Month	Longitude	Latitude
January	86.7	5.1
February	–	–
March	96.1	6.3
April	90.1	10.3
May	90.5	10.4
June	89.0	14.3
July	89.7	19.9
August	–	–
September	91.8	16.9
October	90.1	12.4
November	91.8	9.8
December	87.9	7.3

Further, following the IMD classification, TCs were classified into different categories based on MSW speed (Table 1). However, in this study, TCs were considered when MSW speed is greater than 34 kt. The severe cyclonic storm (SCS), very severe cyclonic storm (VSCS), extremely severe cyclonic storm (ESCS), and super cyclonic storm (SupCS) were together considered as intense cyclonic storms (ICSs). If any TC happens to cross a month or a year, then that cyclone is counted in the previous month or year. Apart from this, all those TCs which formed in the western Pacific and later entered or redeveloped in the BoB were also included in this study.

Alone, the number of TCs during a season may not capture the true impact of that season. Therefore, in this study, ACE (Bell et al. 2000) and PDI (Emanuel 2005) were computed to define the overall TCs activity. The ACE and PDI energy metrics provide more accurate assessments of the strength of the TC season. ACE can be defined as ACE $= \Sigma V_{max}^2$ having units (10^4 kt^2), where V_{max} is the intensity (MSW) of TC. ACE is the sum of V_{max} squared at all 6-hourly periods when

(a) Cyclonic storms

(b) Severe cyclonic storms

(c) Very severe cyclonic storms

(d) Extremely cyclonic storms

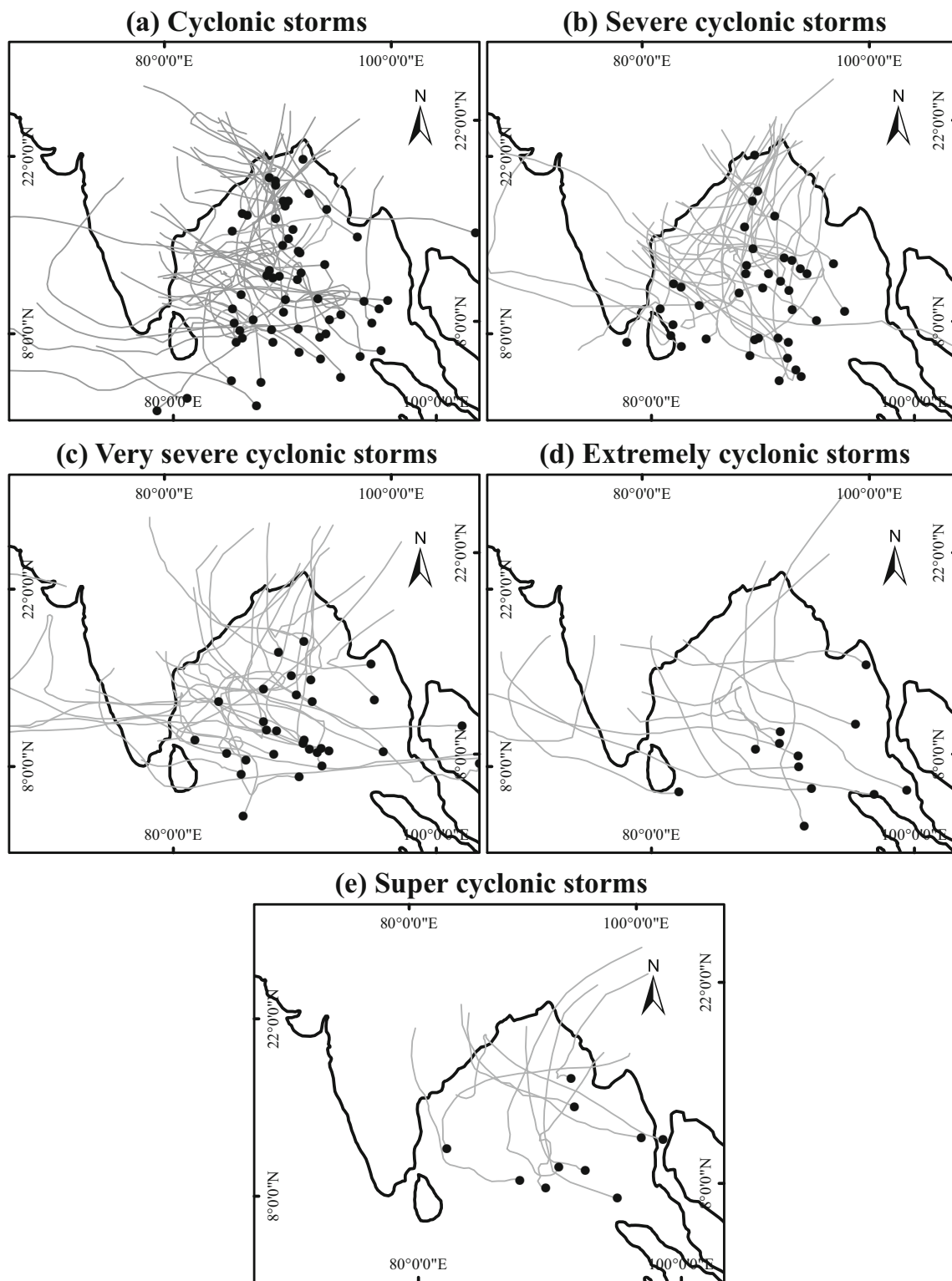## (e) Super cyclonic storms

Fig. 4 Intensity-wise distribution of genesis locations (dots) and tracks (lines) of TCs formed in the BoB during the period 1972–2017. **a** Cyclonic storms, **b** Severe cyclonic storms, **c** Very severe cyclonic storms, **d** Extremely severe cyclonic storms, **e** Super cyclonic storms

the TC is at least of tropical storm strength ($\geq$ 34 kt). The annual ACE was calculated by summing up the ACE of all TCs in a year. PDI, defined as PDI = ΣV_{max}^3 having units (10^6 kt^3), analogous to ACE, is a widely used parameter to characterize the destructive potential of TCs. Both energy metrics take into account the frequency, intensity, and duration of all

Fig. 5 Distribution of number of
TCs by **a** total distance traveled
and **b** intensity-wise mean
distance traveled in the BoB
during the period 1972–2017
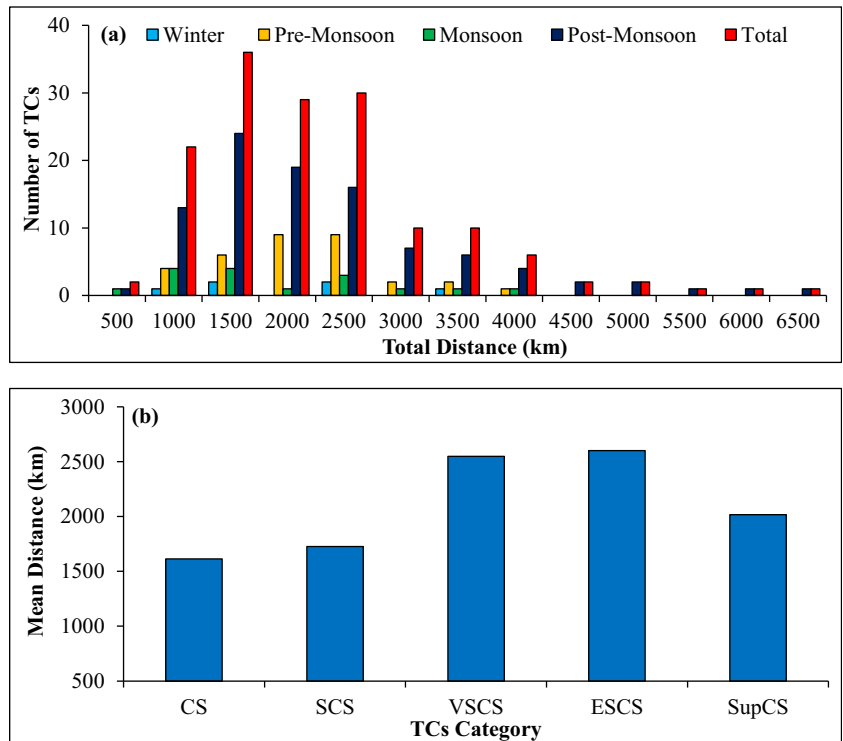
the TCs in a season. ACE and PDI were calculated for each TC during a month, season, and year separately.

Intensification events (increase in MSW of 15 kt in 24 h) and rapid intensification events (increase in MSW of 30 kt in 24 h) were identified using MSW of each TC. The duration of TCs in hours (h) accounts only those 6-hourly periods when MSW is ≥ 34 kt in the lifetime of a TC. For TC days, duration of a TC was divided by 24 and accumulated for the season.

Fig. 6 Annual distribution of **a**
number of TCs and **b** their ACE
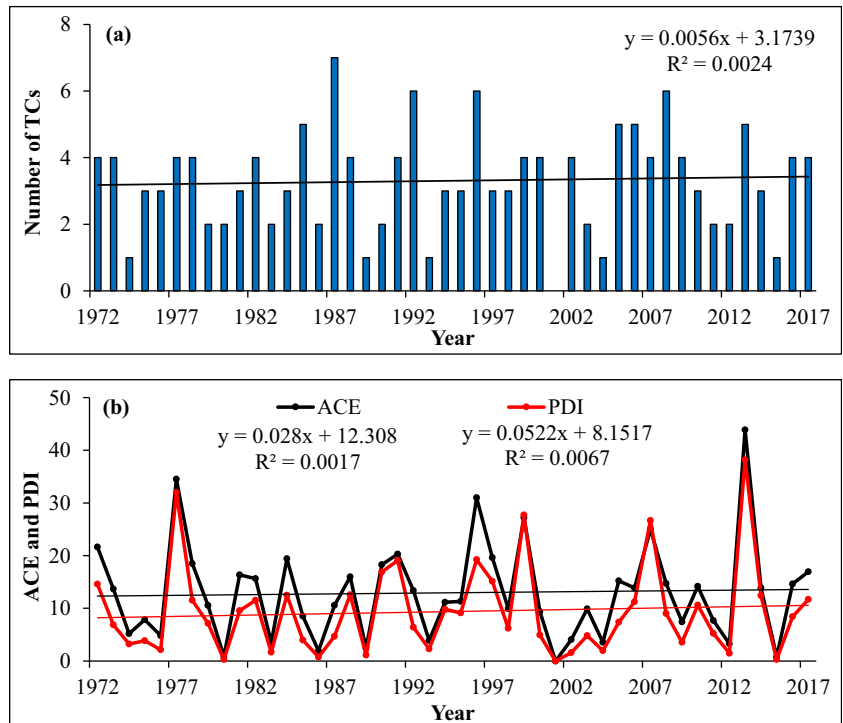and PDI values in the BoB during
the period 1972–2017

Table 3 Mean number of TCs, ACE, and PDI in the BoB during the period 1972–2017

Period	Mean TCs	CV	Mean ACE	CV	Mean PDI	CV
Annual	3.30	46.39	12.97	71.18	9.38	91.50
Winter	0.13	261.05	0.16	269.18	0.06	276.21
Pre-monsoon	0.72	91.35	3.53	134.97	2.64	166.79
Monsoon	0.35	184.01	0.42	268.00	0.22	313.78
Post-monsoon	2.11	64.20	8.85	103.28	6.46	131.55

The total distance traveled by a TC was measured from the first (genesis location) to the last observation point (dissipation) in the dataset. For seasonal analysis, a year was divided into four seasons as per the classification of IMD, namely, winter (January–February), pre-monsoon (March–May), Monsoon (June–September), and post-monsoon (October–December).

To summarize the data, simple descriptive statistics, i.e., sum, percentage, mean, standard deviation (SD), coefficient of variation (CV), were used. Additionally, the Mann-Kendall trend test was performed to identify the trends in the TCs activity (Mann 1945; Kendall 1975). A trend was considered significant if the p value was smaller than 0.05. The correlation analysis was performed by using Karl-Pearson's method. The analyzed data was summarized in the form of tables, graphs, and maps. The maps of genesis locations and tracks of TCs were prepared by using the ArcGIS 10.2.

3 Results and discussion

3.1 Spatial distribution

3.1.1 Annual distribution

Figure 1 exhibits the annual distribution of genesis locations and tracks of TCs formed in the BoB during the 46-year period. The TCs were formed in all the parts of the BoB and made their landfall over the coasts of India, Bangladesh, Myanmar, and Sri Lanka. Only 10% of TCs were dissipated over the BoB basin. Majority of TCs were formed between the 5° N

Fig. 7 **a** Seasonal and **b** monthly distribution of TCs in the BoB during the period 1972–2017. The overlaid black and red curves with dots represent the monthly mean ACE and PDI values, respectively. The values above each bar represent the TC numbers per year in that month
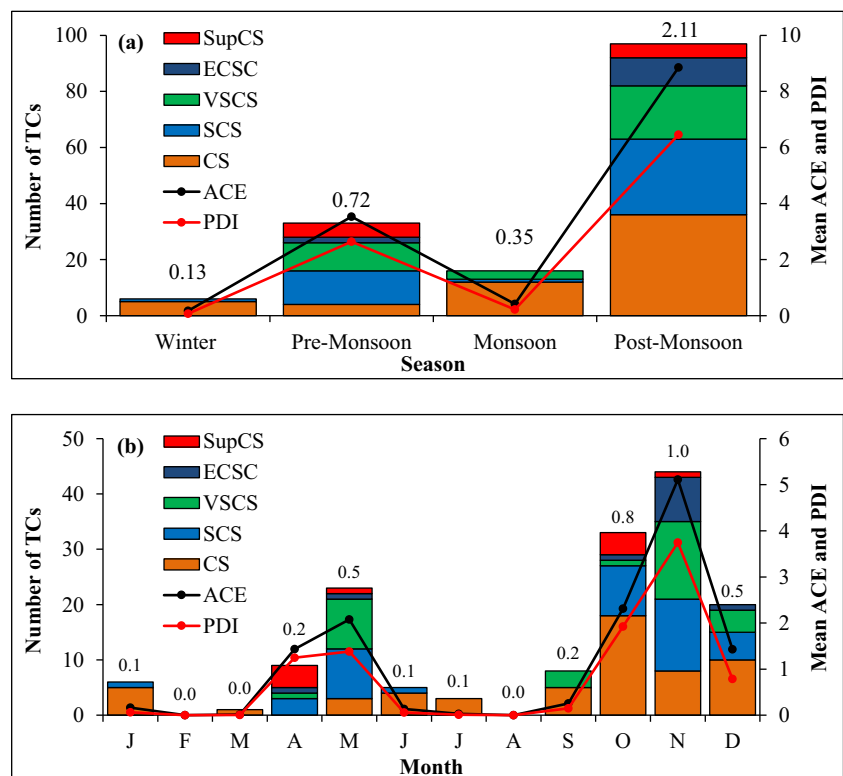
to 16° N latitudes. A few TCs were formed in the lower latitudes (Fig. 2). The TCs formation increases with latitudes and the maximum number of TCs were formed between 8° N to 10° N latitudes. After that, the TCs formation decreases systematically. Similarly, wide variations have been observed in the longitudinal variations in the TCs formation. The maximum number of TCs was formed in the domain of 88° E to 92° E longitudes and TCs formation decreases continuously on both sides of this domain.

3.1.2 Seasonal and monthly distribution

Figure 3a–d shows the seasonal distribution of genesis locations and tracks of TCs in the BoB. During the winter season, the frequency of TCs was very less and formed in southern parts of the BoB and followed the westward track (Fig. 3a). In the pre-monsoon season, the frequency of TCs increases rapidly with a shift in their genesis locations towards north (Fig. 3b). Most of the TCs of this season had followed the northward track and made their landfall over Bangladesh and Myanmar coast. The genesis locations continuously shifted towards north and majority of TCs were formed in the monsoon trough region near the head of the BoB during the monsoon season; however, the TC genesis significantly reduced (Fig. 3c). The TCs of the monsoon season usually cross over the coast of Orissa state of India. During the post-monsoon season, frequency of TCs had increased significantly and was formed in all parts of the BoB (Fig. 3d). The entire eastern coast of India was severely affected by the landfall of TCs during this season.

Figure 3e–p shows the monthly distribution of TCs genesis locations and tracks in the BoB. A large variation in the TCs genesis locations and tracks was witnessed in different months. The mean genesis location of BoB TCs almost followed the northward and southward shifting of Sun (Table 2). The mean genesis location of TCs shifted northward from the month of January to July and then moved southwards continuously, although no TCs were formed during the months of February and August in the BoB during a 46-year study period.

3.1.3 Intensity-wise distribution

Figure 4 exhibits the distribution of the genesis locations and tracks of TCs of different intensities. TCs of different intensity were formed in all the parts of the BoB. Likewise, no definite pattern was observed in their genesis locations and tracks. Although, the majority of CSs, SCSs, and VSCSs were formed in the central parts, while ESCSs and SupCSs were formed in the central-eastern parts of the BoB.

3.1.4 Total distance traveled

Figure 5 shows the total distance traveled by the TCs from the genesis location to dissipation point. Majority of the TCs (approximately 77%) had traveled the distance between 1000 and 2500 km with dual peaks. The first peak was observed between 1000 to 1500 km and the second peak was between 2000 and 2500 km (Fig. 5a). In addition, TCs traveling more than 4000 km distance were far less and formed in the post-monsoon season only. A TC formed in the BoB on October

Table 4 TCs formed in the BoB during the period 1972–2017 for one-third monthly intervals

Month	Date (one-third of a month)	Number of TC	Av. TC per year
January	1–10	2	0.043
January	10–20	2	0.043
January	20–31	2	0.043
February	1–10	0	0.000
February	10–20	0	0.000
February	20–28	0	0.000
March	1–10	0	0.000
March	10–20	1	0.022
March	20–31	0	0.000
April	1–10	1	0.022
April	10–20	2	0.043
April	20–30	6	0.130
May	1–10	7	0.152
May	10–20	9	0.196
May	20–31	7	0.152
June	1–10	1	0.022
June	10–20	2	0.043
June	20–30	2	0.043
July	1–10	1	0.022
July	10–20	0	0.000
July	20–31	2	0.043
August	1–10	0	0.000
August	10–20	0	0.000
August	20–31	0	0.000
September	1–10	3	0.065
September	10–20	3	0.065
September	20–30	2	0.043
October	1–10	7	0.152
October	10–20	11	0.239
October	20–31	15	0.326
November	1–10	17	0.370
November	10–20	15	0.326
November	20–30	12	0.261
December	1–10	11	0.239
December	10–20	5	0.109
December	20–31	4	0.087

14, 1996, had covered the longest distance (approximately 6036 km) during the study period. The mean distance traveled by TCs of the pre- and post-monsoon seasons was approximately 1884 (SD = 698) and 2024 (SD = 1142) km, respectively. Apart from this, Fig. 5b displays that the highest mean distance had been traveled by the ESCSs followed by VSCSs, SupCSs, SCSs, and CSs.

3.2 Temporal distribution

3.2.1 Annual distribution

Figure 6a presents the annual number of TCs during 1972–2017 in the BoB. A total of 152 TCs were formed at the rate of 3.30 cyclones per year, with a SD of 1.53. The interannual variability in the frequency of TCs ranges from 0 (2001) to 7 (1987). However, the trend line did not show any statistically

significant upward and downward trend in the frequency of TCs ($p = 0.748$). The mean annual ACE and PDI value is 12.97 (SD = 9.23) and 9.38 (SD = 8.58), respectively (Table 3). Similar to the TCs frequency, annual ACE and PDI exhibit the large fluctuations with the lowest value in 2001 (0) and maximum in 2013 (44 and 38) (Fig. 6b). Likewise, no statistically significant upward and downward trend was detected in ACE ($p = 0.788$) and PDI ($p = 0.589$).

3.2.2 Seasonal and monthly distribution

Figure 7 shows the seasonal and monthly frequency of TCs and mean ACE and PDI during 1972–2017. The maximum number of TCs was formed during the post-monsoon (about 64%) followed by pre-monsoon (about 21%), monsoon (about 11%), and winter (about 4%) season (Fig. 7a). Annual TCs frequency was strongly correlated with the

Fig. 8 Annual distribution of TCs **a** pre-monsoon and **b** post-monsoon seasons, **c** and **d** shows the ACE and PDI values of pre- and post-monsoon seasons, respectively in the BoB during the period 1972–2017
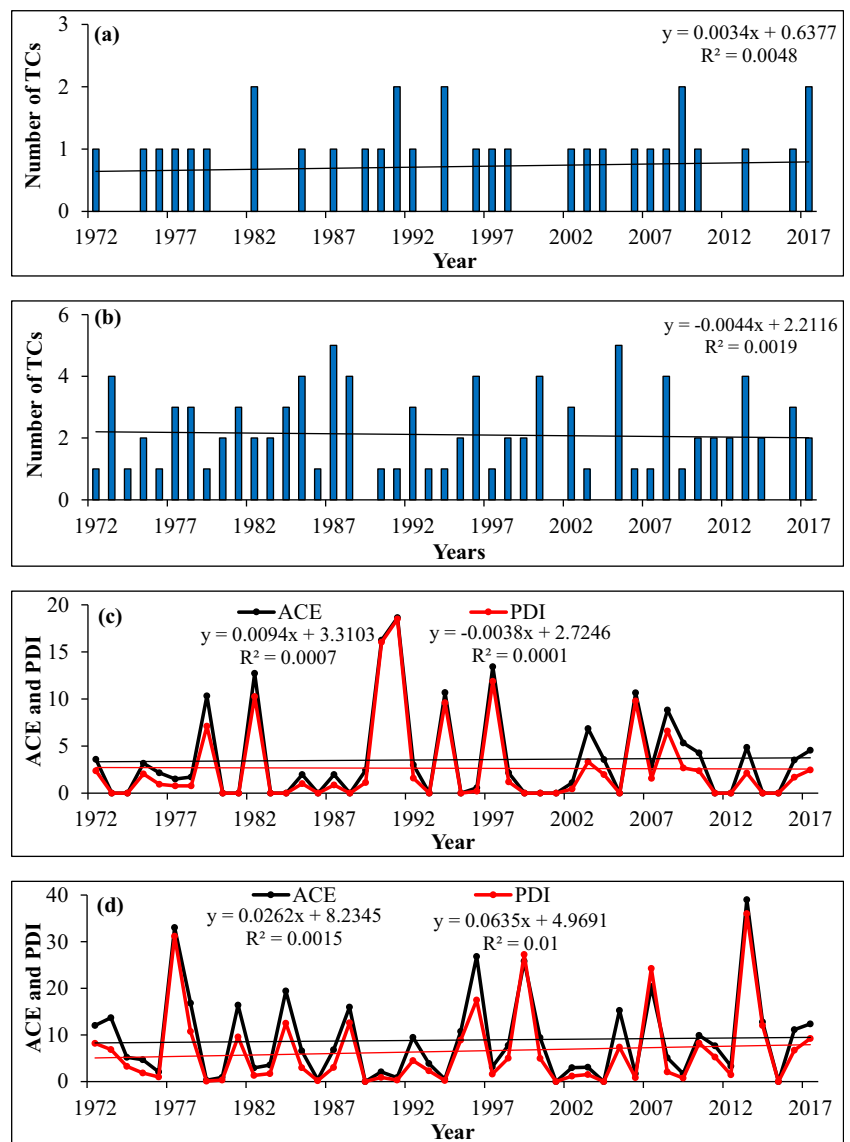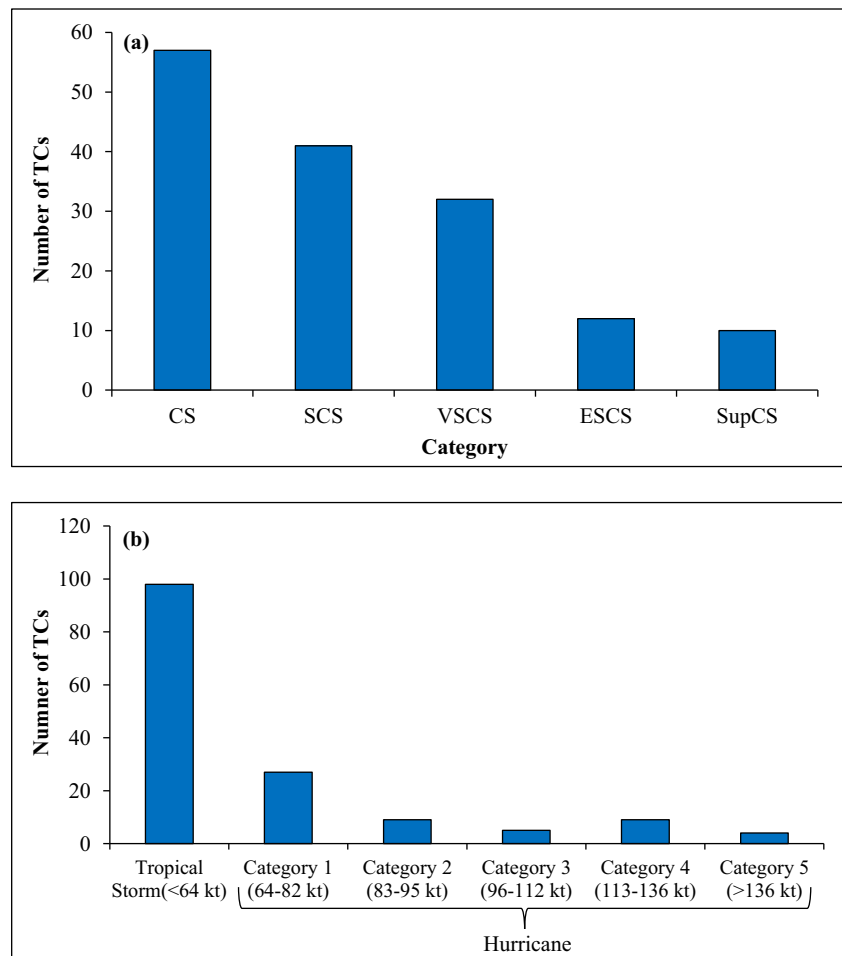
Fig. 9 Intensity-wise number of TCs **a** IMD categorization and **b** Saffir-Simpson Hurricane wind scale in the BoB during the period 1972–2017

post-monsoon season (correlation coefficient value = 0.75, significant at the 99% confidence level). Monthly frequency exhibited a unique bimodal pattern in the occurrence of BoB TCs and their ACE and PDI (Fig. 7b). The first peak was witnessed in the month of May (0.5 TC/year), while the second peak in the month of November (1 TC/year). No TC was formed in February and August.

In addition, a year was divided into 10-day interval to identify the most favored TCs development periods within different months. Table 4 presents the total and mean number of

Table 5 Intensity-wise top ten TCs in the BoB during the period 1972–2017

| Date and year	Duration (h)	MSW (knots)	Equivalent to hurricane category	ACE	PDI
30 April–5 May 1982	132	120	4	9.61	8.77
3–11 May 1990	192	125	4	16.23	16.04
22–30 April 1991	198	140	5	17.56	18.03
26 April–3 May 1994	168	125	4	9.86	9.30
15–18 October 1999	090	120	4	8.29	8.12
25 October–03 November 1999	228	140	5	17.52	19.11
24–29 April 2006	132	120	4	10.66	9.80
10–15 November 2007	132	140	5	20.367	24.26
19–24 October 2010	108	135	4	6.83	6.76
7–13 October 2013	150	140	5	19.80	24.07

TCs formed during different 10-day interval period. First one-third period of November and second one-third period of May had experienced the two peaks in the BoB. Overall, during the pre-monsoon season, most of TCs were formed during the last one-third of the April and the entire month of May. Similarly, during the post-monsoon season, TCs formation was higher in the entire month of October and November and first one-third of December. Thus, these results indicate that approximately 77% of the total TCs were formed in the 11 out of 36 10-day interval periods in a year.

3.2.3 TCs frequency during two peak seasons

Figure 8 shows the annual distribution of TCs during the pre- and post-monsoon season for the period 1972–2017. The mean frequency of TCs during these seasons is 0.72 and 2.11, respectively. A large interannual variability of TCs was observed in the BoB without any significant increasing and decreasing trend during both pre-monsoon ($p = 0.646$) and post-monsoon ($p = 0.774$) seasons (Fig. 8a–b). The ACE and PDI values had also represented large interannual variability with a constant trend during both seasons (Fig. 8c–d). The mean ACE values during the pre- and post-monsoon seasons were observed to be 3.53 and 8.85, respectively. Similarly, the mean PDI values during the pre- and post-monsoon seasons were found to be 2.64 and 6.46, respectively. The mean ACE and PDI values of the post-monsoon season were approximately 68% of the mean annual values.

Fig. 10 Annual distribution of **a** CSs and ISCs, **b** and **c** shows the ACE and PDI values of CSs and ICSs, respectively, **d** shows the MSW speed in the BoB during the period 1972–2017
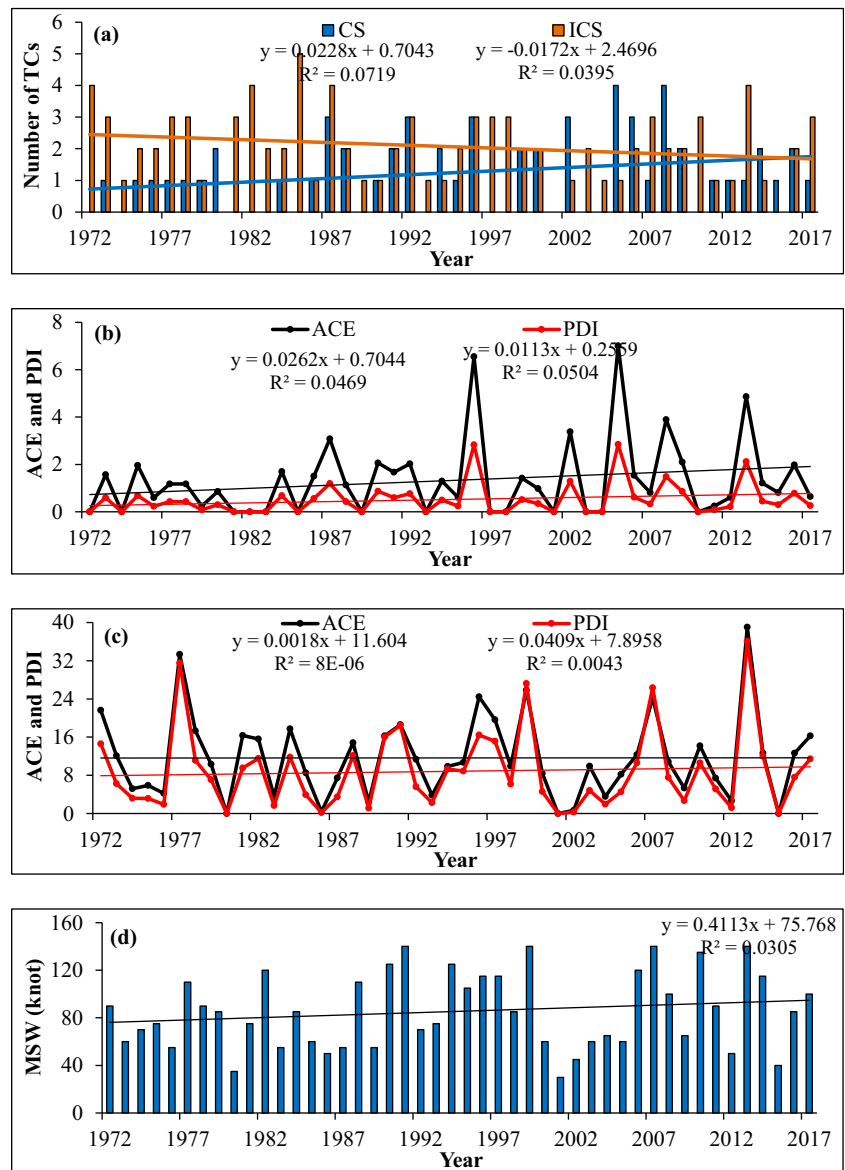
3.3 Intensity of TCs

Figure 9a shows that out of the total 152, the maximum numbers of TCs were of CS intensity (38%), and approximately 27, 21, 8, and 7% TCs reached at the intensity of SCS, VSCS, ESCS, and SupCS, respectively. As per the Saffir-Simpson Hurricane Wind Scale, 54 TCs (approximately 36%) reached at the hurricane category in the BoB (Fig. 9b). Out of these 54 TCs, 27 (50%), 9 (17%), 5 (9%), 9 (17%), and 4 (7%) TCs were of category 1, 2, 3, 4, and 5, respectively during the 46-year study period. Besides, Table 5 shows the top ten TC events in terms of intensity (MSW) formed in the BoB.

On average, 1.24 CSs (MSW 34–47 kt) and 2.06 intense cyclonic storms (ICSs; MSW > 48 kt) were formed every year in the BoB. Interestingly, the number of CSs ($p = 0.071$) and their ACE ($p = 0.148$) and PDI ($p = 0.133$) values showed a slightly non-significant increasing trend (Fig. 10a–b). Conversely, a number of ICSs ($p = 0.186$) showed a slightly

non-significant decreasing trend with constant trend in their ACE ($p = 0.985$) and PDI ($p = 0.665$) values (Fig. 10a and c). This constant trend in ACE and PDI values of ICSs can be attributed to the increasing trend in severity of TCs in terms of MSW speed ($p = 0.246$) (Fig. 10d). Of the total 10 SupCS, 8 occurred in April and October (4 each) and 2 occurred in May and November (1 each). Further, it was observed that the conversion rate of CSs to ICSs (ratio of number of ICSs to the number of total cyclones) is higher during the pre-monsoon (0.88) than post-monsoon (0.63) season. All the TCs of April month were reached at the category of SCSs, VSCSs, ESCSs, and SupCSs (Fig. 7b).

3.4 Intensification and rapid intensification

Intensification and rapid intensification of TCs pose significant operational difficulties (Rappaport et al. 2012; Elsberry 2014; Wang et al. 2017). Since 1972, approximately 40 and

Fig. 11 Distribution of TCs **a** annual duration, **b** duration-wise number, and **c** mean monthly duration in the BoB during the period 1972–2017
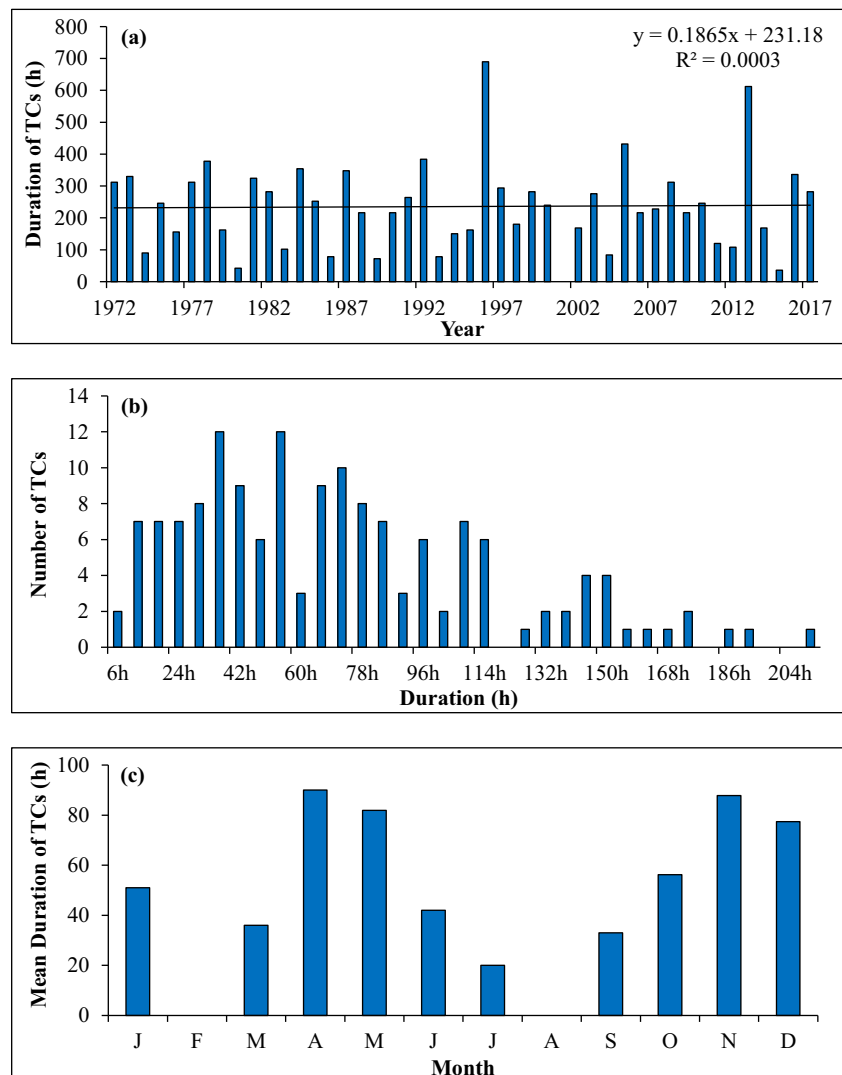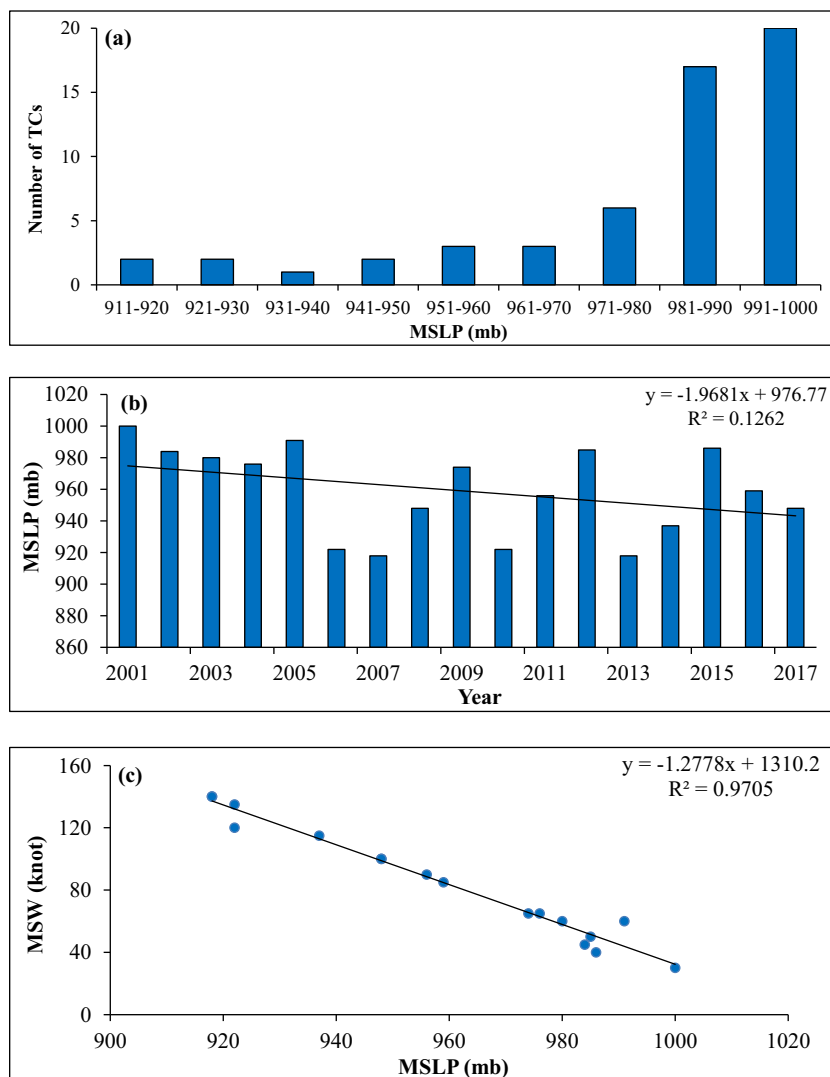
Fig. 12 a Total number of TCs with different MSLP, **b** annual distribution of MSLP, and **c** relationship between the MSW and MSLP in the BoB during the period 1972–2015

3.5 Duration of TCs

The mean annual duration of TCs (h) over BoB was 235.6 h. This means, the number of TCs days per year in the BoB was approximately 10. Figure 11a shows the interannual variability in duration of TCs which ranged from 0 (2001) to 690 (1996) h (SD = 137.6). The mean duration of each TC was approximately 71 h (3 days). The frequency distribution of duration shows that the maximum TCs lie between 12 and 114 h and the long-lasting cyclones are rare (Fig. 11b). In some cases, the TCs last for an extremely long time. For example, on November 26, 1996, a cyclone was formed over the BoB with duration of 210 h (8.8 days) and another cyclone was formed on May 8, 2003, with duration of 192 h (8 days).

Figure 11c reveals that the mean monthly duration of TCs (h) was maximum during the month of April (90 h) followed by November (87.8 h), May (81.9 h), and December (77.4 h). Interestingly, the number of TCs was very less in the month of April; however, their mean duration was very high. The higher mean duration of April TCs can be a major cause for their higher rate of intensification during the pre-monsoon season.

3.6 MSLP and MSW

The mean MSLP during the TCs was approximately 960 mb, ranging from 918 to 1000 mb in the BoB. Majority of the TCs

11% TCs were observed to be intensified and rapidly intensified, respectively in the BoB. These intensification and rapid intensification rates are almost equal to the North Atlantic TCs (Yaukey 2014). The intensification and rapid intensification rates were relatively higher during the pre-monsoon than the post-monsoon season. The maximum magnitude (a 65-kt increase over just 24 h) of rapid intensification was reported for TCs Giri in 2010 and Phailin in 2013.

had MSLP between 980 and 1000 mb (Fig. 12a). MSLP was much lower than 950 mb during the SupCSs and ESCSs. Apart from this, opposite to the trend of MSW speed, the annual distribution of MSLP showed a decreasing trend during the TCs in the BoB ($p = 0.162$) (Fig. 12b). A strong negative correlation (CC = $-$ 0.97) was observed between annual MSLP and MSW (significant at 99% confidence level) (Fig. 12c).

4 Summary and conclusions

The present study is an attempt to develop a long-term climatology of BoB TCs based on JTWC dataset for the period 1972–2017. A total of 152 TCs with an average of 3.30 TCs per year were formed in the BoB without any significant increasing or decreasing trend. Similarly, non-significant increasing or decreasing trends were observed in their ACE and PDI values. The TCs were formed in all parts of the BoB and made their landfall over the coasts of India, Bangladesh, Myanmar, and Sri Lanka. A wide variation in the genesis locations and tracks was observed during two peak TC seasons (pre- and post-monsoon seasons). During the pre-monsoon season, most of the TCs had followed the northward track and made their landfall over Bangladesh and Myanmar coasts, whereas TCs of the post-monsoon season affected the entire coast of BoB. Monthly spatial pattern of BoB TCs exhibited that genesis locations and tracks had almost followed the northward and southward shifting of Sun. The mean genesis location of TCs shifts northward from the month of January to July and then it moves southwards continuously. Majority of the TCs traveled a distance between 1000 and 2500 km, while the mean distance traveled by post-monsoon TCs was higher than the pre-monsoon season. Of the total, approximately 40% and 11% TCs were found to be intensified and rapidly intensified, respectively. The intensification and rapid intensification rates were relatively higher during the pre-monsoon than the post-monsoon season. As per the Saffir-Simpson Hurricane Wind Scale, 54 TCs (approximately 36% of total) were reached at the hurricane category in the BoB. Further, a unique bimodal pattern was observed in monthly occurrence of TCs, ACE, and PDI. The first peak was witnessed in the month of May (0.5 TC/year), while the second in the month of November (1 TC/year). The maximum number of TCs was formed during post-monsoon (approximately 64%), while the lowest during winters (approximately 4%). The mean annual duration of TCs was 235.6 h. The duration of the maximum number of TCs lies between 12 to 114 h, whereas the long-lasting cyclones were rare. Interestingly, the number of CSs and their ACE and PDI values showed a slightly non-significant increasing trend. Conversely, the number of ICSs showed a slightly non-significant decreasing trend with constant trend in their ACE

and PDI values. This constant trend in ACE and PDI values of ICSs can be attributed to the increasing trend in severity of TCs in terms of MSW speed. A significant negative correlation was observed between annual MSLP and MSW. Overall, this study addressed the above-stated research questions in detail and provided comprehensive information pertaining to the long-term climatology of BoB TCs in terms of their annual, seasonal, and monthly spatial and temporal distributions along with their intensity, ACE, PDI, intensification and rapid intensification rates, MSLP, duration, and total distance traveled. The results of this study will update the current knowledge of BoB TCs and may be beneficial for academicians, scientists, and disaster managers.

References

Ali MM, Jagadeesh PSV, Jain S (2007) Effects of eddies on Bay of Bengal cyclone intensity. EOS Trans Am Geophys Union 88:93–95

Bell GD, Halpert MS, Schnell RC, Higgins RW, Lawrimore J, Kousky VE, Tinker R, Thiaw W, Chelliah W, Artusa A (2000) Climate assessment for 1999. Bull Am Meteorol Soc 81:1328

Bhardwaj P, Pattanaik DR, Singh O (2019a) Tropical cyclone activity over Bay of Bengal in relation to El Niño-Southern Oscillation. Int J Climatol. https://doi.org/10.1002/joc.6165

Bhardwaj P, Singh O, Pattanaik DR, Klotzbach PJ (2019b) Modulation of Bay of Bengal tropical cyclone activity by the Madden-Julian oscillation. Atmos Res 229:23–38

Chittibabu PS, Dube K, Macnabb JB, Murty TS, Rao AD, Mohanty UC, Sinha PC (2004) Mitigation of flooding and cyclone hazard in Orissa, India. Nat Hazards 31:455–485

Chowdhury KMMH (2002) Cyclone preparedness and management in Bangladesh. In: BPATC (ed) Improvement of early warning system and responses in Bangladesh towards total disaster risk management approach. BPATC, Dhaka, pp 115–119

Chu JH, Sampson CR, Levine AS, Fukada E 2002 The joint typhoon warning center tropical cyclone best-tracks, 1945–2000. US Naval Research Laboratory Report NRL/MR/7540-02-16, pp 22

Elsberry RL (2014) Advances in research and forecasting of tropical cyclones from 1963–2013. Asia-Pac J Atmos Sci 50:3–16

Emanuel KA (2005) Increasing destructiveness of tropical cyclones over the past 30 years. Nature 436:686–688

Evan AT, Camargo SJ (2011) A climatology of Arabian Sea cyclonic storms. J Clim 24:140–158

Felton CS, Subrahmanyam B, Murty VSN (2013) ENSO-modulated cyclogenesis over the Bay of Bengal. J Clim 26:9806–9818

Frank WM (1987) Tropical cyclone formation. A global view of tropical cyclones, Office of Naval Research, pp 53–90

Fritz HM, Blount CD, Thwin S, Thu MK, Chan N (2009) Cyclone Nargis storm surge in Myanmar. Nat Geosci 2:448–449

Girishkumar MS, Ravichandran M (2012) The influences of ENSO on tropical cyclone activity in the Bay of Bengal during October–December. J Geophys Res 117:C02033

Gray WM (1979) Hurricanes: their formation, structure and likely role in the general circulation. In: Shaw DB (ed) Meteorology over the

tropical oceans. Royal Meteorological Society, James Glaisher House, Grenville Place, Bracknell, Berks, RG 12 1BX, pp 155–218

Gutzler DS, Wood KM, Ritchie EA, Douglas AV, Lewis MD (2013) Interannual variability of tropical cyclone activity along the Pacific coast of North America. Atmosfera 26:149–162

IMD (2011) Tracks of cyclones and depressions over North Indian Ocean (from 1891 onwards) (Cyclone eAtlas - IMD, Version 2.0). Cyclone Warning and Research Centre, India Meteorological Department, Regional Meteorological Centre, Chennai

Kendall MG (1975) Rank correlation methods. Charles Griffin, London

Kikuchi K, Wang B (2010) Formation of tropical cyclones in the northern Indian Ocean associated with two types of tropical intraseasonal oscillation modes. J Meteorol Soc Jpn 88:475–496

Knapp KR, Kruk MC (2010) Quantifying interagency differences in tropical cyclone best-track wind speed estimates. Mon Weather Rev 138:1459–1473

Knapp KR, Kruk MC, Levinson DH, Diamond HJ, Neumann CJ (2010) The International Best Track Archive for Climate Stewardship (IBTrACS): unifying tropical cyclone data. Bull Am Meteorol Soc 91:363–376

Lin I-I, Chen C-H, Pun I-F, Liu WT, Wu C-C (2009) Warm ocean anomaly, air sea fluxes, and the rapid intensification of tropical cyclone Nargis (2008). Geophys Res Lett 36:L03817

Mann HB (1945) Non-parametric tests against trend. Econometrica 13: 245–259

McBride JL (1995) Tropical cyclone formation. In: Elsberry RL (ed) Global perspectives on tropical cyclones, WMO/TD-No. 693, World Meteorological Organization, Geneva, pp 63–105

Neumann CJ (1993) Global overview. In: Global guide to tropical cyclone forecasting. World Meteorological Organization, Geneva, pp 1.1–1.56

Ng EKW, Chan JCL (2012) Interannual variations of tropical cyclone activity over the north Indian Ocean. Int J Climatol 32:819–830

Pattanaik DR (2005) Variability of oceanic and atmospheric conditions during active and inactive periods of storms over the Indian region. Int J Climatol 25:1523–1530

Pattanaik DR, Mohapatra M (2016) Seasonal forecasting of tropical cyclogenesis over the North Indian Ocean. J Earth Syst Sci 132:231–250

Peduzzi P, Chatenoux B, Dao H, Bono AD, Herold C, Kossin J, Mouton F, Nordbeck O (2012) Global trends in tropical cyclone risk. Nat Clim Chang 2:289–294

Pielke RA Jr, Rubiera J, Landsea C, Fernandez ML, Klein R (2003) Hurricane vulnerability in Latin America and the Caribbean: normalized damage and loss potentials. Nat Hazards Rev 4:101–114

Pielke RA Jr, Gratz J, Landsea CW, Collins D, Saunders MA, Musulin R (2008) Normalized hurricane damage in the United States: 1900–2005. Nat Hazards Rev 9:29–42

Rappaport EN, Jiing J-G, Landsea CW, Murillo ST, Franklin JL (2012) The joint hurricane test bed: its first decade of tropical cyclone research-to-operations activities reviewed. Bull Am Meteorol Soc 93:371–380

Rosenfeld D, Woodley WL, Khain A, Cotton WR, Carrio G, Ginis I, Golden JH (2012) Aerosol effects on microstructure and intensity of tropical cyclones. Bull Am Meteorol Soc 93:987–1001

Sengupta D, Goddalehundi BR, Anitha DS (2007) Cyclone induced mixing does not cool SST in the post-monsoon north Bay of Bengal. Atmos Sci Lett 9:1–6

Singh OP (2008) Indian Ocean dipole mode and tropical cyclone frequency. Curr Sci 94:29–31

Singh OP (2010) Recent trends in tropical cyclone activity in the North Indian Ocean. In: Charabi Y (ed) Indian Ocean tropical cyclones and climate change. Springer, Dordrecht, pp 51–54

Singh OP, Khan TMA, Rahman MS (2001) Has the frequency of intense tropical cyclones increased in the north Indian Ocean? Curr Sci 80: 575–580

Wang C, Wang X, Weisberg RH, Black ML (2017) Variability of tropical cyclone rapid intensification in the North Atlantic and its relationship with climate variations. Clim Dyn 49:3627–3645

Yanase W, Satoh M, Taniguchi H, Fujinami H (2012) Seasonal and intraseasonal modulation of tropical cyclogenesis environment over the Bay of Bengal during the extended summer monsoon. J Clim 25: 2914–2930

Yaukey PH (2014) Intensification and rapid intensification of North Atlantic tropical cyclones: geography, time of year, age since genesis, and storm characteristics. Int J Climatol 34:1038–1049

Zhao H, Raga GB (2015) On the distinct interannual variability of tropical cyclone activity over the eastern North Pacific. Atmosfera 28:161–178